ADMM-based Distributed Active and Reactive Power Control for Regional AC Grid with Wind Farms

Wang, Pengda; Wu, Qiuwei; Huang, Sheng; Li, Canbing; Zhou, Bin

Published in:
Journal of Modern Power Systems and Clean Energy

Publication date:
2022

Document Version
Peer reviewed version

ADMM-based Distributed Active and Reactive Power Control for Regional AC Grid with Wind Farms

Pengda Wang, Qiuwei Wu, Sheng Huang, Canbing Li, and Bin Zhou

***Abstract*—A distributed active and reactive power control (DARPC) strategy based on the alternating direction method of multipliers (ADMM) is proposed for regional AC transmission system (TS) with wind farms (WFs). The proposed DARPC strategy optimizes the power distribution among the WFs to minimize the power losses of the AC TS while tracking the active power reference from the transmission system operator (TSO), and minimize the voltage deviation of the buses inside the WF from the rated voltage as well as power losses of the WF collection system. The optimal power flow (OPF) of the TS is relaxed by using the semidefinite programming (SDP) relaxation while the branch flow model is used to model the collection system of the WF. In the DARPC strategy, the large-scale strongly coupled optimization problem is decomposed by using the ADMM, which are solved in the regional TS controller and WF controllers in parallel without loss of the global optimality. The boundary information is exchanged between the regional TS controller and WF controllers. Compared to the conventional OPF method of the TS with WFs, the optimality and accuracy of the system operation can be improved. Moreover, it efficiently reduces the computation burden of the system controller and eliminates the need of a central controller. The protection of the information privacy can be enhanced. A modified IEEE 9-bus system with two WFs consisting of 64 wind turbines (WTs) is used to validate the proposed DARPC strategy.**

***Index Terms*—Alternating direction method of multipliers (ADMM), distributed active and reactive power control (DARPC), OPF, semidefinite programming (SDP), wind farm.**

I. Introduction

WIND power has been continuously developing due to the increasing demand of renewable energy and low-carbon energy policy [1]. With the wind power penetration increasing, the wind power fluctuations and the interaction between large-scale wind farms (WFs) and power systems have introduced several technical challenges, e.g., the optimal power allocation, voltage regulation and coordination for the AC transmission system (TS) with WFs [2].

Optimal power flow (OPF) has been widely used to solve the operation problem of the power system connected WFs. There are a number of papers on OPF-based optimal operation of the power system with WFs [3]-[7]. In [3], a multi-period OPF model was formulated to minimize the operating cost in the grid with offshore WFs. In [4], an OPF-based optimal generation schedule was proposed to minimize the total system cost and operate the system securely with wind power. In [5], an extended OPF model was used to minimize the generation cost of thermal units and wind units in the power system with WFs. In [6], a multi-objective stochastic OPF model was formulated to reduce the operating cost, emission and enhance the voltage stability in the power system with significant wind penetration. In [7], an optimal reactive power dispatch strategy based on OPF was proposed to minimize the voltage stability index in a wind power integrated power system.

For the WF control, the conventional strategy is the proportional distribution (PD) control scheme. The active and reactive power references of wind turbines (WTs) are proportionally distributed according to the available wind power, which is easy to implement [8]. However, the PD control scheme cannot achieve optimal power distribution inside the WF. Several optimization-based dispatch methods have been developed to overcome the disadvantage of the PD scheme and achieve better control performance of the WF. In [9], an optimal power dispatch method was proposed to reduce the production cost and maximize the active power production of the WF. In [10], an optimal active power dispatch strategy was proposed to reduce fatigue loads in WFs with distributed energy storage systems (ESSs). In [11], an optimal reactive power dispatch method was developed to minimize the total losses in the WF.

With the WF expanding both in size and number, if the system operator tries to solve a global optimization problem of the WFs with the TS, it may be difficult to solve a large-scale OPF-based optimization problem with large-scale constraints in seconds. In order to meet the needs of fast calculation of WF dynamic control with strong fluctuations in wind speed, the alternating direction method of multipliers (ADMM) has been applied to

The work was supported in part by Technical University of Denmark (DTU), and in part by China Scholarship Council (No. 201806130202).

P. Wang, Q. Wu (corresponding author) and S. Huang are with the Center for Electric Power and Energy (CEE), Department of Electrical Engineering, Technical University of Denmark (DTU), Kgs. Lyngby 2800, Denmark (e-mail: penwan@elektro.dtu.dk; qw@elektro.dtu.dk; huang98123@163.com).

C. Li is with the School of Electronic Information and Electrical Engineering, Shanghai Jiao Tong University, Shanghai 200240, China (e-mail: licanbing@sjtu.edu.cn).

B. Zhou is with the College of Electrical and Information Engineering, Hunan University, Changsha 410082, China (e-mail: binzhou@hnu.edu.cn).

reduce the computation burden and communication burden of the controller [24], [25]. The ADMM-based optimization methods have been widely used in the WF optimal control [8], [12]-[15]. In [8], an ADMM-based two-tier active and reactive power control scheme was proposed to achieve the optimal voltage regulation inside the WF cluster. In [12], an ADMM-based voltage control method was proposed for the large-scale WF cluster to coordinate the reactive power output among several WFs and WTs inside each WF. In [13], a model predictive control method based on ADMM was proposed to minimize voltage deviations and reactive power output fluctuations of WTs inside WFs. In [14], an ADMM-based optimal active power control method was proposed for synthetic inertial response of large-scale WFs. The aim is to minimize the differences in the rotor speed of the WTs and the wind energy loss.

In the existing studies, there is no study on the optimal power control for the regional TS with WFs while considering the voltage regulation and power loss management inside WFs. With the WF and TS expanding both in size and number, the large amount of wind power from the large-scale WF cluster has to be transported to the bulk power system through a meshed transmission grid. The coordination of the TS and WFs is necessary to achieve optimal operation of the whole system. Therefore, this paper proposes a distributed active and reactive power control (DARPC) strategy based on ADMM for the regional TS with WFs. The proposed strategy aims to achieve the global optimal power control of the regional TS with WFs to minimize the total power losses while meeting the TSO requirements for active power demand, and regulate bus voltages inside each WF within a feasible range. The ADMM method is used to decompose the large-scale optimization problem. The non-convex OPF problem of the TS is relaxed by using semidefinite programming (SDP) relaxation and Schur's complement [18]. Meanwhile, the branch flow model [2] is used to formulate the optimization problem of the WF. With the proposed DARPC strategy, the TS and WF controllers operate in parallel to solve the optimization problem in a distributed manner without loss of global optimality.

The main contribution of this paper can be summarized as follows:

1) A DARPC strategy is developed for the TS with WFs, which can achieve the global optimal power distribution and the voltage regulation for the coupled TS and WFs. The DARPC can achieve a better control performance among the TS and WFs.

2) The SDP relaxation and Schur's complement are adopted for the TS while the branch flow model is adopted for the WFs, which handle the inherent non-convexities of the OPF problem of the coupled TS and WFs. Thus, the original problem is transformed into a convex problem and can be solved using the ADMM framework while guaranteeing the global optimal solution.

3) The ADMM-based DARPC strategy eliminates the requirement of the central controller and distributes the system computation task to several controllers to reduce the computation burden, implying the better scalability. The exchanged information between the TS controller and WF controllers only includes the global, local and dual variables of the boundary nodes, which improves the protection of the information privacy.

The rest of this paper is organized as follows. Section II presents an overview of the proposed DARPC strategy. The TS optimization model and the WF optimization model are formulated in section III and IV, respectively. The distributed solution method based on the ADMM is described in section V. The simulation results and the discussion are presented in section VI, followed by the conclusions.

II. Control Strategy Architecture

A. System Configuration

Figure 1 shows the configuration of AC transmission system connected WFs. Two WFs are connected to a modified IEEE 9-bus system. In the TS, Bus 1 is connected to the 345 kV external power system, and WF1 and WF2 with the nominal power rating of 160 MW are connected to Buses 2 and 3, respectively. Each WF is composed of two sections and each section has a medium voltage (MV) bus. The MV bus is located next to the 155/33 kV substation transformer. Each 33 kV feeder consists of 8 × 5 MW WTs, which are arranged with 4 km away from each other.

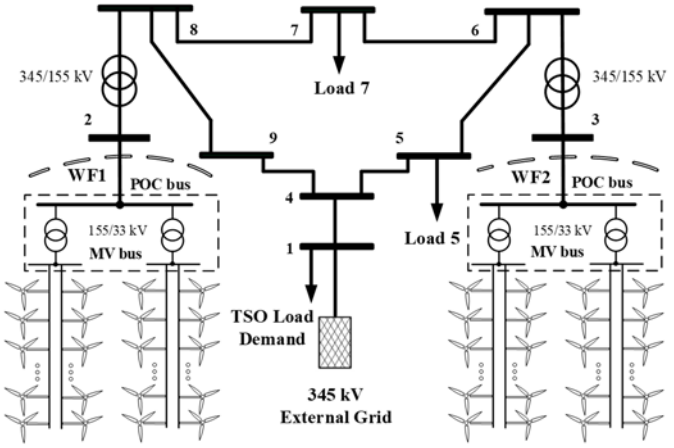

Fig. 1. System configuration.

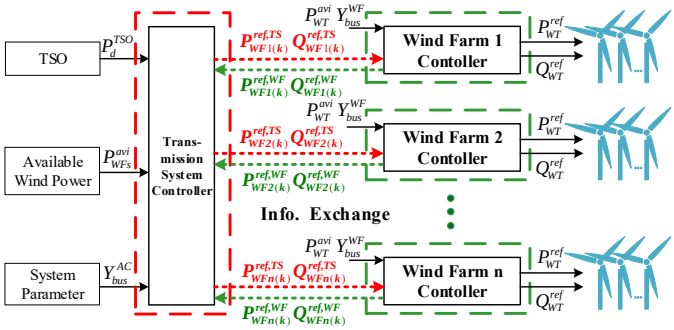

Fig. 2. Concept of proposed strategy.

B. Concept of Proposed Strategy

Figure 2 shows the structure of the proposed strategy. The TS and each WF are equipped with a controller. The whole system operates in a distributed manner by using the ADMM to achieve the global optimal power distribution. The TSO sends the command to the TS controller. The TS controller solves the

optimization problem of the TS to minimize the power losses of the TS and track the active power command from the TSO. Meanwhile, each WF controller generates WT power output references to improve the voltage regulation performance and minimize power losses. The boundary information is exchanged between the TS controller and WF controllers through the communication network. With part of calculation distributed to each WF controller, the large-scale constrained optimization problem is decomposed and the calculation burden can be significantly reduced without loss of the global optimality.

III. Transmission System Optimization Model

A. Objective Function and Constraints

1) Objective function of TS

The objective function is to minimize the total power losses in the TS, which is equal to the total active power generation of WFs minus the total load of the TS. It can also be expressed as the summation of the injected active power into all the buses of the TS. Denoting z^* as the conjugate of an arbitrary complex number z. Thus, the total power losses can be expressed as,

$$\begin{aligned} Obj_{\mathrm{TS}}^{\mathrm{Loss}} &= \sum_{i\in|\mathcal{N}_{\mathrm{TS}}|}(P_{\mathrm{WF}_i}-P_{\mathrm{D}_i}) \\ &= \sum_{i\in|\mathcal{N}_{\mathrm{TS}}|}\mathrm{Re}\{V_i I_i^*\} \end{aligned} \tag{1}$$

where P_{WF_i} is the power output of the i-th WF which is connected to the i-th terminal bus in TS directly; If the bus i is not associated with WF, then $P_{\mathrm{WF}_i}=0$; P_{D_i} denotes the active load at bus i, V_i and I_i are the voltage and current associated with bus i, respectively, and $\mathcal{N}_{\mathrm{TS}}$ is the set of buses in TS.

2) Constraints of TS

The OPF problem of the TS is subjected to a set of equality and inequality constraints. The equality constraints consist of the active/reactive power balance equations,

$$P_{\mathrm{WF}_i}-P_{\mathrm{D}_i}=\mathrm{Re}\{V_i I_i^*\}\ \ \forall i\in\mathcal{N}_{\mathrm{TS}} \tag{2}$$

$$Q_{\mathrm{WF}_i}-Q_{\mathrm{D}_i}=\mathrm{Im}\{V_i I_i^*\}\ \ \forall i\in\mathcal{N}_{\mathrm{TS}} \tag{3}$$

where Q_{WF_i} is the reactive power output of the i-th WF; If the bus i is not associated with WF, then $Q_{\mathrm{WF}_i}=0$.

The inequality constraints are,

$$P_{\mathrm{WF}_i}^{\min}\le P_{\mathrm{WF}_i}\le P_{\mathrm{WF}_i}^{\max} \tag{4}$$

$$Q_{\mathrm{WF}_i}^{\min}\le Q_{\mathrm{WF}_i}\le Q_{\mathrm{WF}_i}^{\max} \tag{5}$$

$$V_i^{\min}\le|V_i|\le V_i^{\max} \tag{6}$$

$$|S_{lm}|\le S_{lm}^{\max} \tag{7}$$

where $|V_i|$ is the voltage magnitude of the i-th terminal bus, S_{lm} is the apparent power flow through the transmission line from bus l to bus m, $P_{\mathrm{WF}i}^{\min}$, $P_{\mathrm{WF}i}^{\max}$, $Q_{\mathrm{WF}i}^{\min}$, $Q_{\mathrm{WF}i}^{\max}$, $V_i^{\min}$ and $V_i^{\max}$ are the lower and upper bounds on the i-th WF active/reactive power outputs, and the i-th terminal bus voltage, respectively; and $S_{lm}^{\max}$ is the maximum value of the apparent power flow through the transmission line (l, m).

B. Convex Relaxation of Optimal Power Flow of TS

In this section, the semidefinite relaxation of the OPF problem of the TS is introduced. With the SDP relaxation applied, the non-convex OPF model of the TS can be transferred to a convex model and then solved under ADMM framework while guaranteeing the global optimal solution. Let matrix Y_{TS} denotes the admittance matrix of TS. For $k\in\mathcal{N}_{\mathrm{TS}}$ and $(l,m)\in Line$, e_k is the k-th basis vector in $R^{|\mathcal{N}_{\mathrm{TS}}|}$, e_k^T is its transposed vector, and $Y_k=\mathrm{e}_k\mathrm{e}_k^T Y_{\mathrm{TS}}$. The π model of the transmission line (l,m) is applied. y_{lm} and $\bar{y}_{lm}$ are used to denote the value of the series and shunt sectors of the line (l,m), respectively [17]. Then $Y_{lm}=(\bar{y}_{lm}+y_{lm})e_l e_l^T-y_{lm}e_l e_m^T$ is defined, which can be expressed as follows,

$$Y_{lm}=\begin{bmatrix} 0 & \cdots & 0 & \cdots & 0 & \cdots & 0 \\ \vdots & & \vdots & & \vdots & & \vdots \\ 0 & \cdots & (\bar{y}_{lm}+y_{lm})_{ll} & \cdots & (-y_{lm})_{lm} & \cdots & 0 \\ \vdots & & \vdots & & \vdots & & \vdots \\ 0 & \cdots & 0 & \cdots & 0 & \cdots & 0 \end{bmatrix}_{|\mathcal{N}_{\mathrm{TS}}|\times|\mathcal{N}_{\mathrm{TS}}|}$$

In order to present the OPF of the TS in SDP form, the matrixes are defined as [17], [19],

$$\mathbf{Y}_k^{\mathrm{TS}}=\frac{1}{2}\begin{bmatrix}\mathrm{Re}(Y_k+Y_k^T) & \mathrm{Im}(Y_k^T-Y_k)\\ \mathrm{Im}(Y_k-Y_k^T) & \mathrm{Re}(Y_k+Y_k^T)\end{bmatrix}$$

$$\overline{\mathbf{Y}}_k^{\mathrm{TS}}=-\frac{1}{2}\begin{bmatrix}\mathrm{Im}(Y_k+Y_k^T) & \mathrm{Re}(Y_k-Y_k^T)\\ \mathrm{Re}(Y_k^T-Y_k) & \mathrm{Im}(Y_k+Y_k^T)\end{bmatrix}$$

$$\mathbf{Y}_{lm}^{\mathrm{TS}}=\frac{1}{2}\begin{bmatrix}\mathrm{Re}(Y_{lm}+Y_{lm}^T) & \mathrm{Im}(Y_{lm}^T-Y_{lm})\\ \mathrm{Im}(Y_{lm}-Y_{lm}^T) & \mathrm{Re}(Y_{lm}+Y_{lm}^T)\end{bmatrix}$$

$$\overline{\mathbf{Y}}_{lm}^{\mathrm{TS}}=-\frac{1}{2}\begin{bmatrix}\mathrm{Im}(Y_{lm}+Y_{lm}^T) & \mathrm{Re}(Y_{lm}-Y_{lm}^T)\\ \mathrm{Re}(Y_{lm}^T-Y_{lm}) & \mathrm{Im}(Y_{lm}+Y_{lm}^T)\end{bmatrix}$$

$$\mathbf{M}_k^{\mathrm{TS}}=\begin{bmatrix}e_k e_k^T & 0\\ 0 & e_k e_k^T\end{bmatrix}$$

The real and imaginary sectors of the complex bus voltage vector $V_{\mathrm{TS}}=[V_1,V_2,\cdots,V_{N_{\mathrm{TS}}}]_{1\times|\mathcal{N}_{\mathrm{TS}}|}$ is used to define $2|\mathcal{N}_{\mathrm{TS}}|\times 1$-dimensional variable vector X_{TS},

$$X_{\mathrm{TS}}=[\mathrm{Re}\{V_{\mathrm{TS}}\}^T\ \mathrm{Im}\{V_{\mathrm{TS}}\}^T]^T_{2|\mathcal{N}_{\mathrm{TS}}|\times 1}$$

Then, the OPF formulation of the TS (1)-(7) with complex variables where the V^*V^T can be substituted with a complex $2|\mathcal{N}_{\mathrm{TS}}|\times 2|\mathcal{N}_{\mathrm{TS}}|$-dimensional matrix W_{TS}, $W_{\mathrm{TS}}=X_{\mathrm{TS}}X_{\mathrm{TS}}^T$. Then the original complex formulation can be split into the real and imaginary parts [17].

$\mathrm{Tr}\{M_a\}$ is used to represent the trace of an arbitrary square matrix M_a. Then, the following (8)-(11) can be used to reformulate the objective function (1) and the constraints (2)-(7) with the new variable matrix W_{TS},

$$\mathrm{Re}\{V_k I_k^*\}=\mathrm{Tr}\{\mathbf{Y}_k^{\mathrm{TS}}W_{\mathrm{TS}}\} \tag{8}$$

$$\mathrm{Im}\{V_k I_k^*\}=\mathrm{Tr}\{\overline{\mathbf{Y}}_k^{\mathrm{TS}}W_{\mathrm{TS}}\} \tag{9}$$

$$(V_k)^2=\mathrm{Tr}\{\mathbf{M}_k^{\mathrm{TS}}W_{\mathrm{TS}}\} \tag{10}$$

$$(S_{lm})^2=\mathrm{Tr}\{\mathbf{Y}_{lm}^{\mathrm{TS}}W_{\mathrm{TS}}\}^2+\mathrm{Tr}\{\overline{\mathbf{Y}}_{lm}^{\mathrm{TS}}W_{\mathrm{TS}}\}^2 \tag{11}$$

1) Transformation of the objective function

To transform the objective function (1) into the SDP form, (8) with the new variable matrix W_{TS} is substituted into original function (1),

$$Obj_{\mathrm{TS,Loss}}^{\mathrm{SDP}} = \sum_{k\in|\mathcal{N}_{\mathrm{TS}}|} \mathrm{Tr}\{\mathbf{Y}_k^{\mathrm{TS}} W_{\mathrm{TS}}\} \tag{12}$$

2) Transformation of the constraints

The active/reactive power balance constraints in (2) and (3) can be combined with the WF active/reactive power output limits in (4) and (5). Then the SDP form of the power balance constraints in terms of the power output limits can be obtained by substituting (8) and (9) into (2) and (3),

$$P_{\mathrm{WF}_k}^{\min} - P_{\mathrm{D}_k} \le \mathrm{Tr}\{\mathbf{Y}_k^{\mathrm{TS}} W_{\mathrm{TS}}\} \le P_{\mathrm{WF}_k}^{\max} - P_{\mathrm{D}_k} \tag{13}$$

$$Q_{\mathrm{WF}_k}^{\min} - Q_{\mathrm{D}_k} \le \mathrm{Tr}\{\overline{\mathbf{Y}}_k^{\mathrm{TS}} W_{\mathrm{TS}}\} \le Q_{\mathrm{WF}_k}^{\max} - Q_{\mathrm{D}_k} \tag{14}$$

Similarly, substituting (10) into (6), the voltage constraint can be transformed into the SDP form,

$$(V_k^{\min})^2 \le \mathrm{Tr}\{\mathbf{M}_k^{\mathrm{TS}} W_{\mathrm{TS}}\} \le (V_k^{\max})^2 \tag{15}$$

Substituting (11) into (7), the transmission line capacity constraint can be presented as,

$$\mathrm{Tr}\{\mathbf{Y}_{lm}^{\mathrm{TS}} W_{\mathrm{TS}}\}^2 + \mathrm{Tr}\{\overline{\mathbf{Y}}_{lm}^{\mathrm{TS}} W_{\mathrm{TS}}\}^2 \le (S_{lm}^{\max})^2 \tag{16}$$

In the SDP form, the constraints should be linear in W_{TS}. However, the constraint (16) is expressed as a quadratic constraint of matrix W_{TS}. Thus, the Schur's complement is applied to transform the quadratic apparent line flow constraint (16) into a linear matrix inequality constraint as,

$$\begin{bmatrix} (S_{lm}^{\max})^2 & \mathrm{Tr}\{\mathbf{Y}_{lm}^{\mathrm{TS}} W_{\mathrm{TS}}\} & \mathrm{Tr}\{\overline{\mathbf{Y}}_{lm}^{\mathrm{TS}} W_{\mathrm{TS}}\} \\ \mathrm{Tr}\{\mathbf{Y}_{lm}^{\mathrm{TS}} W_{\mathrm{TS}}\} & 1 & 0 \\ \mathrm{Tr}\{\overline{\mathbf{Y}}_{lm}^{\mathrm{TS}} W_{\mathrm{TS}}\} & 0 & 1 \end{bmatrix} \succeq 0 \tag{17}$$

At the same time, the non-convex constraint $W_{\mathrm{TS}} = X_{\mathrm{TS}} X_{\mathrm{TS}}^T$ can be expressed as,

$$W_{\mathrm{TS}} \succeq 0 \tag{18}$$

$$rank(W_{\mathrm{TS}}) = 1 \tag{19}$$

The convex relaxation is obtained by dropping the rank constraint (19), transforming the non-linear, non-convex OPF of the TS into a convex semidefinite program [18]. If the rank of W_{TS} obtained from the SDP relaxation is 1, then W_{TS} is the global optimum of the original non-linear, non-convex OPF of the TS [18]. Thus, the SDP relaxation of the OPF problem of the TS is as follows,

Minimize Objective function (12)
Subject to Constraints (13) - (18).

The optimization problem is implemented in MATLAB using the optimization toolbox YALMIP and the SDP solver MOSEK [19]. By solving the OPF problem of the TS in SDP form, the TS boundary variables of the optimal active/reactive power references of two WFs $\mathrm{Tr}\{Y_{\mathrm{WF1}}^{\mathrm{TS}} W_{\mathrm{TS}}\}/\mathrm{Tr}\{\bar{Y}_{\mathrm{WF1}}^{\mathrm{TS}} W_{\mathrm{TS}}\}$ and $\mathrm{Tr}\{Y_{\mathrm{WF2}}^{\mathrm{TS}} W_{\mathrm{TS}}\}/\mathrm{Tr}\{\bar{Y}_{\mathrm{WF2}}^{\mathrm{TS}} W_{\mathrm{TS}}\}$ are generated. These boundary variables can be exchanged between TS and WF controllers under ADMM framework.

IV. Wind Farm Optimization Model

Since a WF has a radial topology, the power flow in the WF can be expressed by the linearized branch flow model [16], [21]-[23]. The power flow from the AC TS to the WF is defined as the positive direction in WF collection system,

$$-\mathrm{Tr}\{\mathbf{Y}_{\mathrm{WF}_k}^{\mathrm{TS}} W_{\mathrm{TS}}\} = P_{\mathrm{WF}_k}^{\mathrm{ref,WF}},\ P_j + p_{j+1}^{\mathrm{WT}} = P_{j+1} \tag{20}$$

$$-\mathrm{Tr}\{\overline{\mathbf{Y}}_{\mathrm{WF}_k}^{\mathrm{TS}} W_{\mathrm{TS}}\} = Q_{\mathrm{WF}_k}^{\mathrm{ref,WF}},\ Q_j + q_{j+1}^{\mathrm{WT}} = Q_{j+1} \tag{21}$$

$$V_{j+1} = V_j - \frac{R_j^{\mathrm{WF}} P_j + X_j^{\mathrm{WF}} Q_j}{V_0^{\mathrm{WF}}} \tag{22}$$

where $\mathrm{Tr}\{Y_{\mathrm{WF}_k}^{\mathrm{TS}} W_{\mathrm{TS}}\}/\mathrm{Tr}\{\bar{Y}_{\mathrm{WF}_k}^{\mathrm{TS}} W_{\mathrm{TS}}\}$ and $P_{\mathrm{WF}_k}^{ref,\mathrm{WF}}/Q_{\mathrm{WF}_k}^{ref,\mathrm{WF}}$ are the boundary optimization variables of the active/reactive power outputs for k-th WF processed in TS and WF controllers; $P_j + \boldsymbol{i}Q_j$ is the apparent power flowing from bus j to bus $j+1$, and $(j, j+1) \in Line$; p_{j+1}^{WT} and q_{j+1}^{WT} are the active and reactive power generated by the WT associated with bus $j+1$; V_j is the voltage magnitude at bus j; $R_j^{\mathrm{WF}} + \boldsymbol{i}X_j^{\mathrm{WF}}$ is the complex impedance between bus j and bus $j+1$; Considering the capacity of each WF is much less than the TS, the bus 2 and bus 3 can be assumed as the slack buses for two WFs, respectively; V_0^{WF} is the voltage magnitude at the boundary bus associated with WF.

The per unit voltage variation should also be considered,

$$V_j^{\min} \le V_j \le V_j^{\max} \tag{23}$$

where $V_j^{\min}$ and $V_j^{\max}$ are generally set to 0.95 p.u. and 1.05 p.u., respectively.

To minimize the power losses in each WF collection system, the power losses can be expressed as,

$$Obj_{\mathrm{WF}}^{\mathrm{Loss}} = \sum_{j=1}^{N_{\mathrm{WT}}} (p_j^{\mathrm{WT}}) - P_{\mathrm{WF}_k}^{\mathrm{ref,WF}} \tag{24}$$

The voltage variation for all buses inside WF should also be minimized,

$$Obj_{\mathrm{WF}}^{\mathrm{VD}} = \sum_{j=1}^{N_{\mathrm{WF}}} \left(V_j - V_{\mathrm{rated}}\right)^2 \tag{25}$$

where N_{WF} is the number of the buses in WF, V_{rated} is the rated voltage in WF.

The active power output of each WT should be dispatched as close as possible to the PD-based reference [20],

$$Obj_{\mathrm{WF}}^{\mathrm{PD}} = \sum_{j=1}^{N_{\mathrm{WT}}} (p_j^{\mathrm{WT}} - p_{\mathrm{PD},j}^{\mathrm{ref}})^2 \tag{26}$$

The PD reference is defined as,

$$p_{\mathrm{PD},j}^{\mathrm{ref}} = \frac{P_{\mathrm{WT},j}^{\mathrm{avi}}}{\sum_j P_{\mathrm{WT},j}^{\mathrm{avi}}} P_{\mathrm{WF}}^{\mathrm{ref}} \tag{27}$$

where $P_{\mathrm{WT},j}^{\mathrm{avi}}$ is the available wind power of the j-th WT.

The WF optimization problem can be converted to a standard quadratic-programming (QP) problem and efficiently solved by QP solvers in milliseconds [1]. Thus, the WF optimization problem is as follows,

Minimize Objective function (24) - (26).
Subject to Constraints (20) - (23).

V. ADMM Formulation For Whole System

Considering the whole system consists of the TS and the several WFs with several hundreds or even thousands of WTs, the optimization problem of the whole system becomes a large-scale model with the large-scale constraints. To reduce the computation burden, a DARPC strategy based on the ADMM is proposed. The whole system can be partitioned into several areas: the TS area and two WF areas. With the ADMM algorithm implemented, the calculation of the TS and the WFs can be decoupled. Thus, the objective functions (12) and (24)-(26) can be distributed to the TS controller and WF controllers and processed in parallel while guaranteeing the global optimality. The optimization problem of the whole system is,

$$\begin{aligned}\min\quad & \sum_{k=1}^{|\mathcal{N}_{\mathrm{TS}}|}\mathrm{Tr}\{\mathbf{Y}_{\mathbf{k}}^{\mathrm{TS}}W_{\mathrm{TS}}\}+\sum_{k=1}^{2}\left\{\sum_{j=1}^{N_{\mathrm{WT}}}(p_{j,k}^{\mathrm{WT}})-P_{\mathrm{WF}_k}^{\mathrm{ref,WF}}+\right.\\ & \left.\sum_{j=1}^{N_{\mathrm{WF}}}\left(V_{j,k}-V_{\mathrm{rated}}\right)^2+\sum_{j=1}^{N_{\mathrm{WT}}}(p_{j,k}^{\mathrm{WT}}-p_{\mathrm{PD},j,k}^{\mathrm{ref}})^2\right\}\\ \text{s.t.}\quad & (13)-(18),\quad (20)-(23),\qquad (28)\\ & \mathrm{Tr}\{\mathbf{Y}_{\mathrm{WF}_k}^{\mathrm{TS}}W_{\mathrm{TS}}\}-P_{\mathrm{WF}_k}^{\mathrm{ref,WF}}=0,\ k=1,2.\\ & \mathrm{Tr}\{\overline{\mathbf{Y}}_{\mathrm{WF}_k}^{\mathrm{TS}}W_{\mathrm{TS}}\}-Q_{\mathrm{WF}_k}^{\mathrm{ref,WF}}=0,\ k=1,2.\\ & \mathrm{Tr}\{\mathbf{M}_{\mathrm{WF}_k}^{\mathrm{TS}}W_{\mathrm{TS}}\}-(V_k^{\mathrm{WF}})^2=0,\ k=1,2.\qquad (29)\end{aligned}$$

where $\mathrm{Tr}\{M_{\mathrm{WF}_k}^{\mathrm{TS}}W_{\mathrm{TS}}\}$ and $(V_k^{\mathrm{WF}})^2$ are the square of the k-th boundary bus voltage processed in the TS and WF controllers, respectively. Thus, the argumented Lagrangian of (28) can be expressed as,

$$\begin{aligned}\min\quad & \sum_{k=1}^{|\mathcal{N}_{\mathrm{TS}}|}\mathrm{Tr}\{\mathbf{Y}_{\mathbf{k}}^{\mathrm{TS}}W_{\mathrm{TS}}\}+\sum_{k=1}^{2}\left\{\sum_{j=1}^{N_{\mathrm{WT}}}(p_{j,k}^{\mathrm{WT}})-P_{\mathrm{WF}_k}^{\mathrm{ref,WF}}+\right.\\ & \left.\sum_{j=1}^{N_{\mathrm{WF}}}\left(V_{j,k}-V_{\mathrm{rated}}\right)^2+\sum_{j=1}^{N_{\mathrm{WT}}}(p_{j,k}^{\mathrm{WT}}-p_{\mathrm{PD},j,k}^{\mathrm{ref}})^2\right\}\\ & +\sum_{k=1}^{2}\lambda_k^{\mathrm{P}}[\mathrm{Tr}\{\mathbf{Y}_{\mathrm{WF}_k}^{\mathrm{TS}}W_{\mathrm{TS}}\}-P_{\mathrm{WF}_k}^{\mathrm{ref,WF}}]+\sum_{k=1}^{2}\frac{\rho}{2}\left\|\mathrm{Tr}\{\mathbf{Y}_{\mathrm{WF}_k}^{\mathrm{TS}}W_{\mathrm{TS}}\}-P_{\mathrm{WF}_k}^{\mathrm{ref,WF}}\right\|^2\\ & +\sum_{k=1}^{2}\lambda_k^{\mathrm{Q}}[\mathrm{Tr}\{\overline{\mathbf{Y}}_{\mathrm{WF}_k}^{\mathrm{TS}}W_{\mathrm{TS}}\}-Q_{\mathrm{WF}_k}^{\mathrm{ref,WF}}]+\sum_{k=1}^{2}\frac{\rho}{2}\left\|\mathrm{Tr}\{\overline{\mathbf{Y}}_{\mathrm{WF}_k}^{\mathrm{TS}}W_{\mathrm{TS}}\}-Q_{\mathrm{WF}_k}^{\mathrm{ref,WF}}\right\|^2\end{aligned}\qquad (30)$$

where the dual variables are defined as λ_k^P and λ_k^Q for the objective function. The parameter ρ is considered as the penalty for the optimization variables in the TS that differ from the variables in the WFs.

The system communication network topology is shown in Fig. 3.

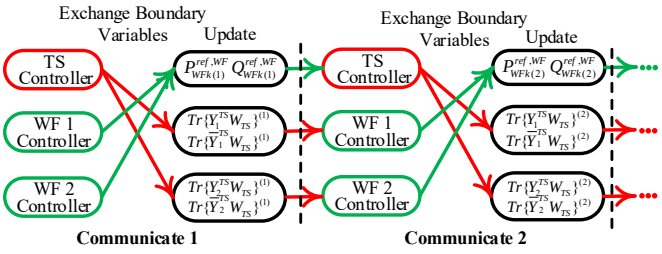

Fig. 3. The system communication network.

The initial optimization variables and the dual variables are set to zero. r is defined as the step of iteration, and each iterative step includes the following steps:

1) The TS controller updates and solves the optimization variables in the TS by using the augmented Lagrangian objective function with the constraints of the TS, and it updates the optimization variables,

$$\begin{aligned}&\left(\mathrm{Tr}\{\mathbf{Y}_{\mathrm{WF}_k}^{\mathrm{TS}}W_{\mathrm{TS}}\},\mathrm{Tr}\{\overline{\mathbf{Y}}_{\mathrm{WF}_k}^{\mathrm{TS}}W_{\mathrm{TS}}\}\right)(r+1)=\underset{\substack{\mathrm{Tr}\{\mathbf{Y}_{\mathrm{WF}_k}^{\mathrm{TS}}W_{\mathrm{TS}}\}\\ \mathrm{Tr}\{\overline{\mathbf{Y}}_{\mathrm{WF}_k}^{\mathrm{TS}}W_{\mathrm{TS}}\}}}{\arg\min}\sum_{k=1}^{|\mathcal{N}_{\mathrm{TS}}|}\mathrm{Tr}\{\mathbf{Y}_{\mathbf{k}}^{\mathrm{TS}}W_{\mathrm{TS}}\}+\\ &\sum_{k=1}^{2}\lambda_k^{\mathrm{P}}[\mathrm{Tr}\{\mathbf{Y}_{\mathrm{WF}_k}^{\mathrm{TS}}W_{\mathrm{TS}}\}-P_{\mathrm{WF}_k}^{\mathrm{ref,WF}}(r)]+\sum_{k=1}^{2}\frac{\rho}{2}\left\|\mathrm{Tr}\{\mathbf{Y}_{\mathrm{WF}_k}^{\mathrm{TS}}W_{\mathrm{TS}}\}-P_{\mathrm{WF}_k}^{\mathrm{ref,WF}}(r)\right\|^2+\\ &\sum_{k=1}^{2}\lambda_k^{\mathrm{Q}}[\mathrm{Tr}\{\overline{\mathbf{Y}}_{\mathrm{WF}_k}^{\mathrm{TS}}W_{\mathrm{TS}}\}-Q_{\mathrm{WF}_k}^{\mathrm{ref,WF}}(r)]+\sum_{k=1}^{2}\frac{\rho}{2}\left\|\mathrm{Tr}\{\overline{\mathbf{Y}}_{\mathrm{WF}_k}^{\mathrm{TS}}W_{\mathrm{TS}}\}-Q_{\mathrm{WF}_k}^{\mathrm{ref,WF}}(r)\right\|^2\end{aligned}\qquad (31)$$

s.t. (13)-(18), (29).

In (31), the augmented Lagrangian objective function is expressed as a quadratic function of matrix W_{TS}. However, in the SDP form, the objective should be linear with W_{TS}. Thus, the objective (32) and constraints (33)-(34) are formulated to represent the original augmented Lagrangian objective (31) using the Schur's complement with auxiliary variables α_k^{P} and α_k^{Q},

$$\begin{aligned}&\left(\mathrm{Tr}\{\mathbf{Y}_{\mathrm{WF}_k}^{\mathrm{TS}}W_{\mathrm{TS}}\},\mathrm{Tr}\{\overline{\mathbf{Y}}_{\mathrm{WF}_k}^{\mathrm{TS}}W_{\mathrm{TS}}\}\right)(r+1)=\\ &\underset{\substack{\mathrm{Tr}\{\mathbf{Y}_{\mathrm{WF}_k}^{\mathrm{TS}}W_{\mathrm{TS}}\}\\ \mathrm{Tr}\{\overline{\mathbf{Y}}_{\mathrm{WF}_k}^{\mathrm{TS}}W_{\mathrm{TS}}\}}}{\arg\min}\sum_{k=1}^{|\mathcal{N}_{\mathrm{TS}}|}\mathrm{Tr}\{\mathbf{Y}_{\mathbf{k}}^{\mathrm{TS}}W_{\mathrm{TS}}\}+\sum_{k=1}^{2}(\alpha_k^{\mathrm{P}}+\alpha_k^{\mathrm{Q}})\end{aligned}\qquad (32)$$

$$\begin{bmatrix}\lambda_k^{\mathrm{P}}\mathrm{Tr}\{\mathbf{Y}_{\mathrm{WF}_k}^{\mathrm{TS}}W_{\mathrm{TS}}\}+a_k^{\mathrm{P}} & \sqrt{\frac{\rho}{2}}\mathrm{Tr}\{\mathbf{Y}_{\mathrm{WF}_k}^{\mathrm{TS}}W_{\mathrm{TS}}\}+b_k^{\mathrm{P}}\\ \sqrt{\frac{\rho}{2}}\mathrm{Tr}\{\mathbf{Y}_{\mathrm{WF}_k}^{\mathrm{TS}}W_{\mathrm{TS}}\}+b_k^{\mathrm{P}} & -1\end{bmatrix}\preceq 0,k=1,2.\qquad (33)$$

$$\begin{bmatrix}\lambda_k^{\mathrm{Q}}\mathrm{Tr}\{\overline{\mathbf{Y}}_{\mathrm{WF}_k}^{\mathrm{TS}}W_{\mathrm{TS}}\}+a_k^{\mathrm{Q}} & \sqrt{\frac{\rho}{2}}\mathrm{Tr}\{\overline{\mathbf{Y}}_{\mathrm{WF}_k}^{\mathrm{TS}}W_{\mathrm{TS}}\}+b_k^{\mathrm{Q}}\\ \sqrt{\frac{\rho}{2}}\mathrm{Tr}\{\overline{\mathbf{Y}}_{\mathrm{WF}_k}^{\mathrm{TS}}W_{\mathrm{TS}}\}+b_k^{\mathrm{Q}} & -1\end{bmatrix}\preceq 0,k=1,2.\qquad (34)$$

s.t. (13)-(18), (29).

where $a_k^{\mathrm{P}}=-\alpha_k^{\mathrm{P}}-\lambda_k^{\mathrm{P}}P_{\mathrm{WF}_k}^{\mathrm{ref,WF}}(r)$, $b_k^{\mathrm{P}}=-\sqrt{\frac{\rho}{2}}P_{\mathrm{WF}_k}^{\mathrm{ref,WF}}(r)$,

$a_k^{\mathrm{Q}}=-\alpha_k^{\mathrm{Q}}-\lambda_k^{\mathrm{Q}}Q_{\mathrm{WF}_k}^{\mathrm{ref,WF}}(r)$, $b_k^{\mathrm{Q}}=-\sqrt{\frac{\rho}{2}}Q_{\mathrm{WF}_k}^{\mathrm{ref,WF}}(r)$.

2) After updating the optimization variables in the TS, each WF controller solves its augmented Lagrangian problem with the constraints of the WF in parallel, and updates the optimization variables. For the k-th WF controller,

$$\begin{aligned}&\left(P_{\mathrm{WF}_k}^{\mathrm{ref,WF}},Q_{\mathrm{WF}_k}^{\mathrm{ref,WF}}\right)(r+1)=\underset{P_{\mathrm{WF}_k}^{\mathrm{ref,WF}},Q_{\mathrm{WF}_k}^{\mathrm{ref,WF}}}{\arg\min}\\ &\sum_{j=1}^{N_{\mathrm{WT}}}(p_{j,k}^{\mathrm{WT}})-P_{\mathrm{WF}_k}^{\mathrm{ref,WF}}+\sum_{j=1}^{N_{\mathrm{WF}}}\left(V_{j,k}-V_{\mathrm{rated}}\right)^2+\sum_{j=1}^{N_{\mathrm{WT}}}(p_{j,k}^{\mathrm{WT}}-p_{\mathrm{PD},j,k}^{\mathrm{ref}})^2+\\ &\lambda_k^{\mathrm{P}}[\mathrm{Tr}\{\mathbf{Y}_{\mathrm{WF}_k}^{\mathrm{TS}}W_{\mathrm{TS}}\}(r+1)-P_{\mathrm{WF}_k}^{\mathrm{ref,WF}}]+\frac{\rho}{2}\left\|\mathrm{Tr}\{\mathbf{Y}_{\mathrm{WF}_k}^{\mathrm{TS}}W_{\mathrm{TS}}\}(r+1)-P_{\mathrm{WF}_k}^{\mathrm{ref,WF}}\right\|^2+\\ &\lambda_k^{\mathrm{Q}}[\mathrm{Tr}\{\overline{\mathbf{Y}}_{\mathrm{WF}_k}^{\mathrm{TS}}W_{\mathrm{TS}}\}(r+1)-Q_{\mathrm{WF}_k}^{\mathrm{ref,WF}}]+\frac{\rho}{2}\left\|\mathrm{Tr}\{\overline{\mathbf{Y}}_{\mathrm{WF}_k}^{\mathrm{TS}}W_{\mathrm{TS}}\}(r+1)-Q_{\mathrm{WF}_k}^{\mathrm{ref,WF}}\right\|^2\\ &k=1,2.\end{aligned}\qquad (35)$$

s.t. (20)-(23), (29).

These two sub-optimization problems can be solved quickly by using the commercial optimization solvers.

3) Update the dual variables in the WF controllers,

$$\lambda_k^{\mathrm{P}}(r+1)=\lambda_k^{\mathrm{P}}(r)+\rho[P_{\mathrm{WF}_k}^{\mathrm{ref,WF}}(r+1)-\mathrm{Tr}\{\Upsilon_{\mathrm{WF}_k}^{\mathrm{TS}}W_{\mathrm{TS}}\}(r+1)] \quad (36)$$

$$\lambda_k^{\mathrm{Q}}(r+1)=\lambda_k^{\mathrm{Q}}(r)+\rho[Q_{\mathrm{WF}_k}^{\mathrm{ref,WF}}(r+1)-\mathrm{Tr}\{\overline{\Upsilon}_{\mathrm{WF}_k}^{\mathrm{TS}}W_{\mathrm{TS}}\}(r+1)] \quad (37)$$

With the part of the computation tasks distributed to each WF controller, the large-scale constrained optimization problem is decomposed. For the TS controller, the computation task is to deal with the objective function with the constraints inside the TS. Considering the several WFs are connected to the TS, the computation burden of the TS controller can be significantly reduced, and meanwhile the central controller and centralized communication can also be eliminated without loss of global optimality. For each WF controller, the computation task is an optimization problem with the constraints inside the WF and its computation burden is not heavy.

VI. Case Study

A. Test System

The WFs with 64 × 5 MW WTs with a modified IEEE-9 bus system are used to demonstrate the performance of the proposed DARPC strategy. For the optimal control strategy, it is carried out every 5 s. In order to examine the performance of the proposed scheme, the simulation results are compared with the centralized active and reactive power control (CARPC) strategy and the ones with active and reactive power proportional distribution (PD) control strategy [12]. In the CARPC strategy, the central controller can generate the active and reactive power references of each WT among WFs and achieve the optimal control performance [8].

B. Control Performance

The total simulation time is 600 s. Fig. 4 shows the available wind power for each WF. The available wind power fluctuates 120-153 MW and 90-120 MW in WF1 and WF2, respectively. During t = 200-400 s, the available wind power gradually rises. After t = 400 s, the available wind power gradually decreases.

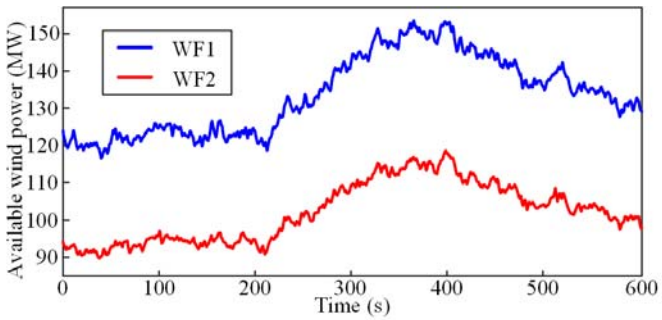

Fig. 4. WF available wind power.

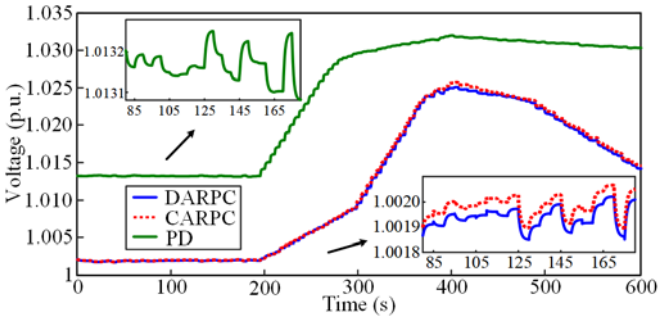

Fig. 5. MV bus 4 voltage in WF1.

The MV bus voltage in WF1 is shown in Fig.5. It can be seen that the DARPC strategy with the ADMM has the similar control performance as the CARPC strategy and they can both effectively control the MV bus voltage within the feasible range. The MV bus voltage is closer to the rated value using DARPC or CARPC than using PD method. The MV bus voltage with DARPC or CARPC can be kept at 1.0019 p.u., and then gradually increases to 1.0250 p.u. with the active power output of WF1 increased by 11.10 MW during t = 200-400 s. After 400 s, the MV bus voltage decreases slightly to 1.0140 p.u. with the active power output decreased by 5.00 MW. Obviously, the voltage value difference between the DARPC and CARPC strategies is very small (less than 0.0005 p.u.). Meanwhile, the voltages with these two strategies also exhibit the similar variations.

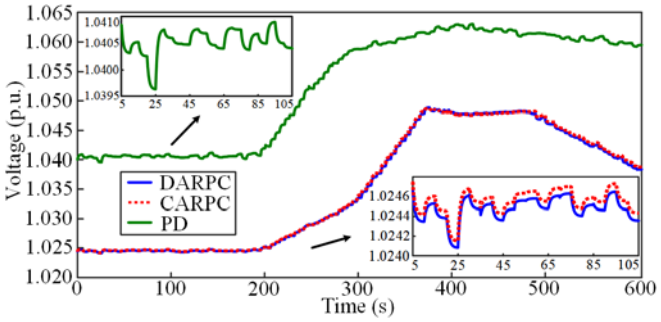

Fig. 6. WT32 terminal voltage in WF1.

Figure 6 shows the WT32 terminal voltage performance, which is located at the furthest position along the feeder in WF1. The performance with the DARPC and CARPC strategies is very similar and much better than PD method. During the whole control period, the WT32 terminal voltage can be kept within 1.024-1.048 p.u., while the voltage with PD method is farther away from the rated value. The voltage deviation with the DARPC or CARPC is also better than PD method. The maximal voltage difference between the DARPC and CARPC strategies is 0.00008 p.u.

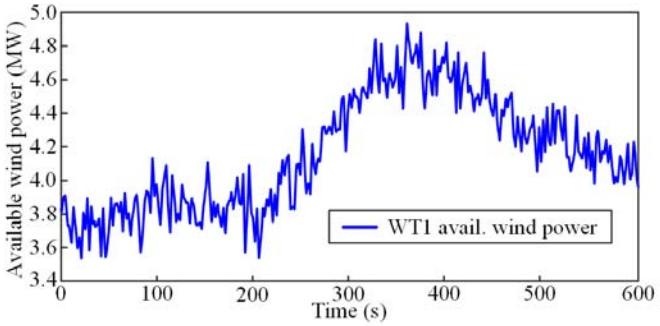

Fig. 7. WT1 available wind power in WF1.

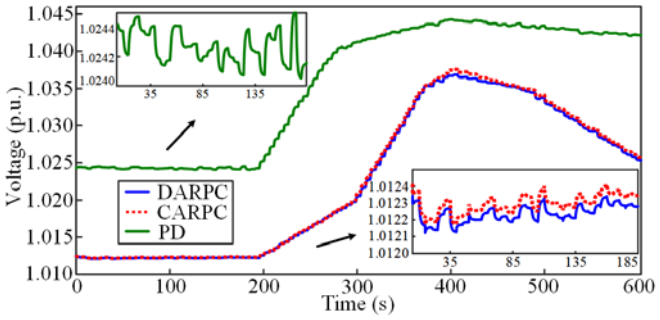

Fig. 8. WT1 terminal voltage in WF1.

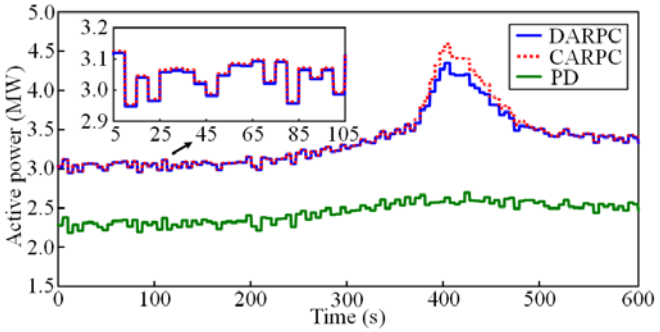

Fig. 9. WT1 output active power in WF1.

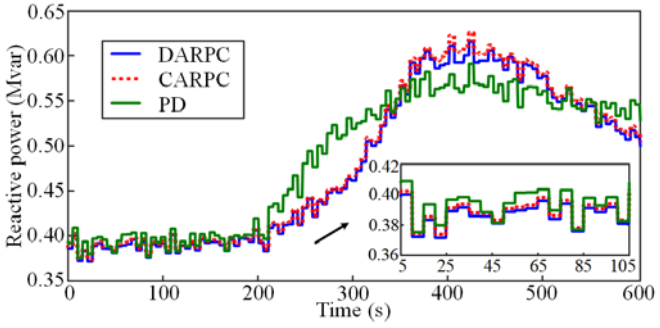

Fig. 10. WT1 output reactive power in WF1.

WT1 is selected as the representative WT in WF1 to illustrate the performance of the WF control among three control strategies. In Figs. 7-10, during t = 200-400 s, the WT1 terminal voltage with DARPC or CARPC gradually increases from 1.0123 p.u. to 1.0368 p.u. with the WT1 active and reactive power output increasing 1.37 MW and 0.2025 Mvar. The WT1 terminal voltage is closer to the rated value, and the voltage fluctuation is also smaller using DARPC or CARPC than using PD method. Obviously, the DARPC and CARPC on the voltage regulation, active and reactive power output are very similar and show better control performance than PD method.

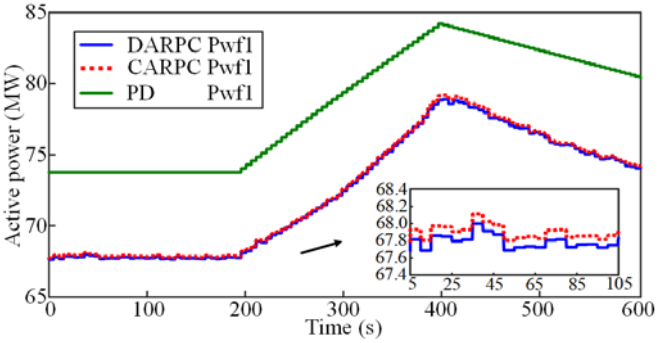

Fig. 11. WF1 output active power.

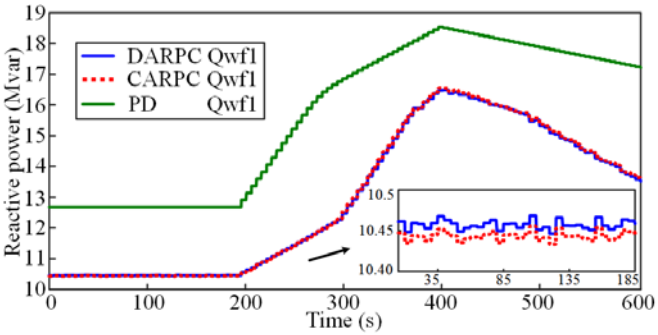

Fig. 12. WF1 output reactive power.

The active and reactive power outputs of WF1 are presented in Figs. 11-12. The active and reactive power output of WF1 with DARPC is very similar with CARPC, and different from the PD method.

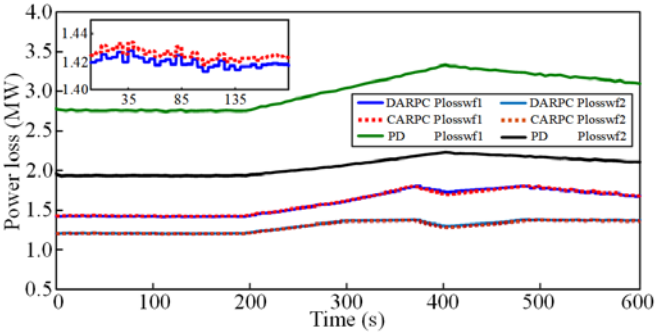

Fig. 13. Power loss of WF1/WF2.

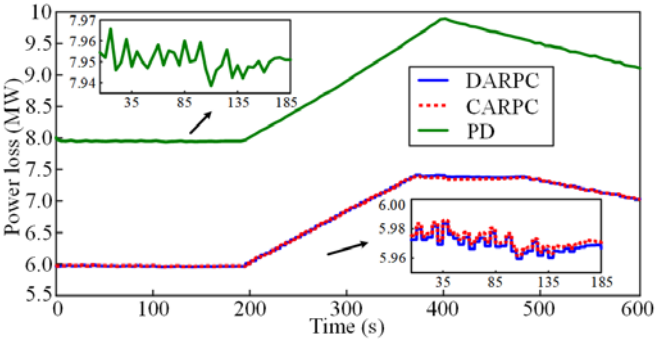

Fig. 14. Power loss of the whole system.

The power losses for WF2, WF3 and the whole system are shown in Figs. 13-14, respectively. As these figures shown, the power losses with DARPC and CARPC are very similar, and much better than PD method. Meanwhile, compared with the CARPC strategy, the distributed control strategy eliminates the central controller and largely reduces the computation burden

and communication cost. Moreover, since each WF controller only exchanges the very little boundary information with the TS controller, the protection of information and data privacy is evidently improved.

Figures 15-17 show the convergence performance of the system. The boundary information of the active and reactive power outputs of WF1 and WF2 are selected to illustrate the results. The TS and WF optimization variables with the active power output for WF1 and WF2 converge to the same value and keep steady after 13 iterations. The convergence performance is acceptance. As Fig. 17 shown, the TS and WF optimization variables with the reactive power output for WF1 and WF2 converge to 10.46 Mvar and 14.08 Mvar in 13 iterations, which shows the excellent convergence performance.

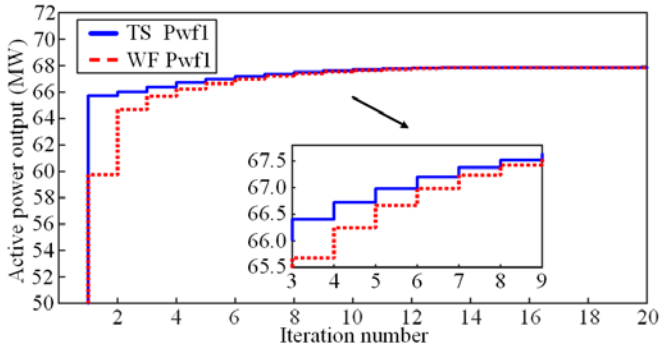

Fig. 15. Convergence performance of active power output of WF1. (t=20s)

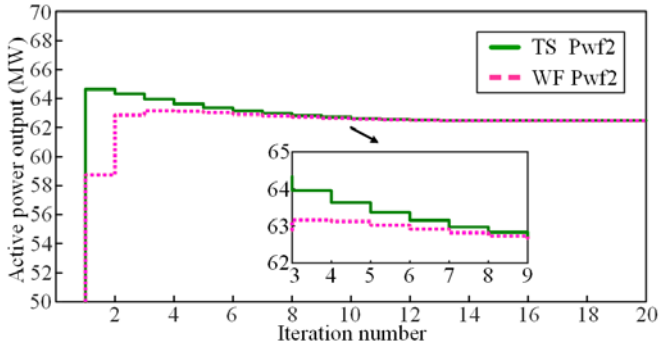

Fig. 16. Convergence performance of active power output of WF2. (t=20s)

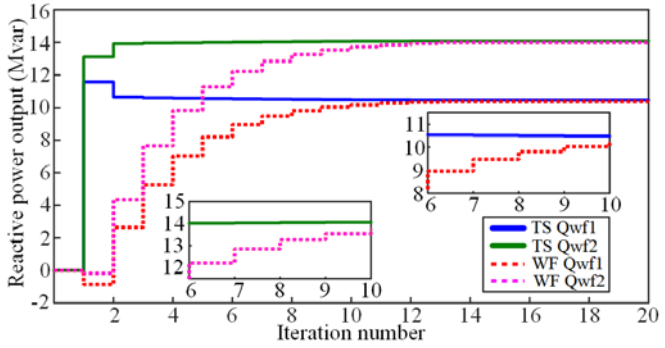

Fig. 17. Convergence performance of reactive power output of WFs. (t=20s)

VII. Conclusion

In this paper, the DARPC strategy based on the ADMM is proposed for the regional AC TS with WFs. The SDP relaxation with Schur's complement and branch flow model are adopted to address the nonconvexity and nonlinearity issues of the global optimal power distribution in the coupled TS and WFs. The ADMM is applied to decompose the large-scale strongly coupled optimization problem without loss of global optimality. The computation burden can be largely reduced with the DARPC strategy. Furthermore, the TS and WF controllers process in parallel only with the limited boundary information exchange, which improves information privacy of the whole system. As verified by the case studies, the proposed DARPC strategy can achieve the optimal power distribution among the WFs to minimize the power losses of the TS while minimizing the voltage deviation of the terminal buses as well as the power losses of the WF collection system.

References

[1] Y. Guo, H. Gao, Q. Wu *et al*., "Enhanced voltage control of VSC-HVDC-connected offshore wind farms based on model predictive control," *IEEE Transactions on Sustainable Energy*, vol. 9, no. 1, pp. 474-487, Jan. 2018.

[2] S. Huang, P. Li, Q. Wu *et al*., "ADMM-based distributed optimal reactive power control for loss minimization of DFIG-based wind farms," *International Journal of Electrical Power and Energy Systems*, vol. 118, Jun. 2020.

[3] A. Rabiee and A. Soroudi, "Stochastic multiperiod OPF model of power systems with HVDC-connected intermittent wind power generation," *IEEE Transactions on Power Delivery*, vol. 29, no. 1, pp. 336-344, Feb. 2014.

[4] A. Panda and M. Tripathy, "Optimal power flow solution of wind integrated power system using modified bacteria foraging algorithm," *International Journal of Electrical Power and Energy Systems*, vol. 54, no. 1, pp. 306-314, Jan. 2014.

[5] L. Xie, H. D. Chiang, and S. H. Li, "Optimal power flow calculation of power system with wind farms," in *Proceedings of 2011 IEEE PES General Meeting*, Detroit, USA, Jul. 2011, pp. 1-6.

[6] M. B. Wafaa and L. A. Dessaint, "Multi-objective stochastic optimal power flow considering voltage stability and demand response with significant wind penetration," *IET Generation, Transmission & Distribution*, vol. 11, no. 14, pp. 3499-3509, Sept. 2017.

[7] S. M. Mohseni-Bonab, A. Rabiee, and B. Mohammadi-Ivatloo, "Voltage stability constrained multi-objective optimal reactive power dispatch under load and wind power uncertainties: A stochastic approach," *Renewable Energy*, vol. 85, pp. 598-609, Jan. 2016.

[8] S. Huang, Y. Gong, Q. Wu *et al*., "Two-tier combined active and reactive power control for VSC-HVDC connected large-scale wind farm cluster based on ADMM," *IET Renewable Power Generation*, vol. 14, no. 8, pp.1379-1386, Jun. 2020.

[9] P. Hou, W. Hu, B. Zhang *et al*., "Optimised power dispatch strategy for offshore wind farms," *IET Renewable Power Generation*, vol. 10, no. 3, pp. 399-409, Mar. 2016.

[10] S. Huang, Q. Wu, Y. Guo *et al*., "Hierarchical active power control of DFIG-based wind farm with distributed energy storage systems based on ADMM," *IEEE Transactions on Sustainable Energy*, vol. 113, no. 3, pp. 154-163, Jul. 2020.

[11] B. Zhang, P. Hou, W. Hu *et al*., "A reactive power dispatch strategy with loss minimization for a DFIG-based wind farm," *IEEE Transactions on Sustainable Energy*, vol. 7, no. 3, pp. 914-923, Jul. 2016.

[12] S. Huang, Q. Wu, Y. Guo *et al*., "Distributed voltage control based on ADMM for large-scale wind farm cluster connected to VSC-HVDC," *IEEE Transactions on Sustainable Energy*, vol. 11, no. 2, pp. 584-594, Apr. 2020.

[13] Y. Guo, H. Gao, H. Xing *et al*., "Decentralized coordinated voltage control for VSC-HVDC connected wind farms based on ADMM," *IEEE Transactions on Sustainable Energy*, vol. 10, no. 2, pp. 800-810, Apr. 2019.

[14] S. Huang, Q. Wu, W. Bao *et al*., "Hierarchical optimal control for synthetic inertial response of wind farm based on ADMM," *IEEE Transactions on Sustainable Energy*, doi: 10.1109/TSTE.2019.2963549.

[15] D. Xu, Q. Wu, B. Zhou *et al*., "Distributed multi-energy operation of coupled electricity, heating and natural gas networks," *IEEE Transactions on Sustainable Energy*, doi: 10.1109/TSTE.2019.2961432.

[16] H. G. Yeh, D. F. Gayme, and S. H. Low, "Adaptive VAR control for distribution circuits with photovoltaic generators," *IEEE Transactions on Power Systems*, vol. 27, no. 3, pp. 1656-1663, Aug. 2012.
[17] S. Bahrami, F. Therrien, V. W. S. Wong *et al*., "Semidefinite relaxation of optimal power flow for AC-DC grids," *IEEE Transactions on Power Systems*, vol. 32, no. 1, pp. 289-304, Jan. 2017.
[18] J. Lavaei and S. H. Low, "Zero duality gap in optimal power flow problem," *IEEE Transactions on Power Systems*, vol. 27, no. 1, pp. 92-107, Feb. 2012.
[19] A. Venzke and S. Chatzivasileiadis, "Convex relaxations of probabilistic AC optimal power flow for interconnected AC and HVDC grids," *IEEE Transactions on Power Systems*, vol. 34, no. 4, pp. 2706-2718, Jul. 2019.
[20] S. Huang, Q. Wu, Y. Guo *et al*., "Bi-level decentralized active and reactive power control for large-scale wind farm cluster," *International Journal of Electrical Power and Energy Systems*, vol. 111, pp. 201-215, Oct. 2019.
[21] S. Cai, Y. Xie, Q. Wu *et al*., "Robust MPC-based microgrid scheduling for resilience enhancement of distribution system," *International Journal of Electrical Power and Energy Systems*, vol. 121, Oct. 2020.
[22] F. Shen, J. C. Lopez, Q. Wu *et al*., "Distributed self-healing scheme for unbalanced electrical distribution systems based on alternating direction method of multipliers," *IEEE Transactions on Power Systems*, vol. 35, no. 3, pp. 2190-2199, May. 2020.
[23] R. Li, W. Wei, S. Mei *et al*., "Participation of an energy hub in electricity and heat distribution markets: An MPEC approach," *IEEE Transactions on Smart Grid,* vol. 10, no. 4. pp. 3641-3653, Jul. 2019.
[24] Q. Zhou, M. Shahidehpour, A. Paaso *et al*., "Distributed control and communication strategies in networked microgrids," *IEEE Communications Surveys & Tutorials*, vol. 22, no. 4, pp. 2586-2633, Sept. 2020.
[25] Q. Zhou, Z. Tian, M. Shahidehpour *et al*., "Optimal consensus-based distributed control strategy for coordinated operation of networked microgrids," *IEEE Transactions on Power Systems*, vol. 35, no. 3, pp. 2452–2462, May. 2020.

Pengda Wang received the B.E. degree in electrical engineering from Hefei University of Technology, Hefei, China, in 2014, and the M.E. degree in electrical engineering from Hunan University, Changsha, China, in 2018. He is currently pursuing the Ph.D. degree in electrical engineering from Technical University of Denmark (DTU), Kgs. Lyngby, Denmark. His research interests include coordinated control of wind power and combined AC/DC grid.

Qiuwei Wu obtained the PhD degree in Power System Engineering from Nanyang Technological University, Singapore, in 2009. He was a senior R&D engineer with VESTAS Technology R&D Singapore Pte Ltd from Mar. 2008 to Oct. 2009. He is an Associate Professor at Department of Electrical Engineering, Technical University of Denmark (DTU) since Nov. 2009. He was a visiting scholar at Department of Industrial Engineering & Operations Research (IEOR), University of California, Berkeley, from Feb. 2012 to May 2012 funded by Danish Agency for Science, Technology and Innovation (DASTI), Denmark. He was a visiting scholar at School of Engineering and Applied Sciences, Harvard University from Nov. 2017 to Oct. 2018. His research area is power system operation and control with high renewables, including wind power modelling and control, active distribution networks, and integrated energy systems. He is an Editor of IEEE Transactions on Power Systems and IEEE Power Engineering Letters. He is also an Associate Editor of International Journal of Electrical Power and Energy Systems, Journal of Modern Power Systems and Clean Energy, IET Renewable Power Generation, and IET Generation, Transmission & Distribution.

Sheng Huang received the B.Eng., MSc. and Ph.D. degree in College of Electrical and Information Engineering, Hunan University, Changsha, China, in 2209, 2012 and 2016, respectively. He is currently a Professor with College of Electrical and Information Engineering, Hunan University. His research interests include renewable energy generation, modeling and integration study of wind power, control of energy storage system, and voltage control.

Canbing Li received the B.Eng. and Ph.D. degree from Tsinghua University, Beijing, China, in 2001 and 2006, respectively, both in electrical engineering. He is currently a professor with the School of Electronic Information and Electrical Engineering, Shanghai Jiao Tong University. His research interests include power systems, smart grid, renewable energy, with an emphasis on large-scale power system dispatch, economic and secure operation of power systems, energy efficiency and energy saving in smart grid, electric demand management of data centers, vehicle-to-grid technologies.

Bin Zhou received the B.E. degree in electrical engineering from Zhengzhou University, Zhengzhou, China, in 2006, the M.Eng. degree in electrical engineering from South China University of Technology, Guangzhou, China, in 2009, and the Ph.D. degree from Hong Kong Polytechnic University, Hong Kong, in 2013. Now, he is an Associate Professor in the College of Electrical and Information Engineering, Hunan University, Changsha, China. His research interests include smart grid operation and planning, renewable energy generation, and energy efficiency.